Vibrational properties of a continuous self-similar structure

A. Petri*
Consiglio Nazionale delle Ricerche (CNR), Istituto di Acustica "O.M.Corbino," Via Cassia 1216, 00189 Roma, Italy

A. Alippi, A. Bettucci, F. Craciun, and F. Farrelly
Consiglio Nazionale delle Ricerche (CNR), Istituto di Acustica "O.M.Corbino," Via Cassia 1216, 00189 Roma, Italy and Dipartimento di Energetica, Università di Roma "La Sapienza," Via Scarpa 14, 00161 Roma, Italy

E. Molinari
Consiglio Nazionale delle Ricerche (CNR), Istituto di Acustica "O.M.Corbino," Via Cassia 1216, 00189 Roma, Italy and Dipartimento di Fisica, Università di Modena, Via Campi, 213/a, 41100 Modena, Italy
(Received 22 September 1993; revised manuscript received 29 November 1993)

We present an extensive investigation of the normal modes of vibration of a prototype hierarchical continuous system, consisting of a Cantor-like sequence of piezoelectric and resin elements. From a detailed analysis of the density of states, displacement profiles, and eigenvalue-spacing distributions, evidence is found for the existence of multiple fracton and phonon regimes. The role of resonant modes and the effect of disorder, which may be of primary importance in real systems, are also discussed in detail.

I. INTRODUCTION

The dynamical behavior of self-similar and hierarchical structures has been the subject of extensive study in the last decade, as these can be rather handy models for pointing out the relevant properties of systems lacking translational invariance. Investigations were further expanded on model fractal structures once it was recognized that self-similarity is much more common in nature than previously believed.[1]

An interesting question concerns the vibrational properties of these structures. Work on the spatial behavior and the frequency spectrum of localized modes, usually called *fractons*,[2,3] show a power law behaviour in the density of states (DOS). Moreover, strictly self-similar (deterministic) fractals and hierarchical models exhibit some features somewhere in between those of translationally invariant systems and of disordered systems; e.g., they possess eigenmodes that are neither extended in the usual sense nor exponentially localized, thus giving rise to anomalous transport properties.

Despite the existing results, a more detailed picture of these systems is desirable. Experimental investigations on silica aerogels, which have statistically self-similar structure, have been performed using various complementary scattering techniques,[4] showing evidence for the power law behavior of the low frequency DOS, and for the existence of localized modes. However, with such techniques the localization of modes is only indirectly deduced from the scaling of the DOS.

In order to directly observe the vibrational spectrum of self-similar systems, we have constructed layered macroscopic heterostructures, based on piezoelectric and polymeric materials (composites), with a geometry inspired by that of a Cantor set. We have measured the vibrational frequency spectrum and displacement profiles in the range 10 kHz – 5 MHz, and compared the results with numerical predictions and with existing theories on self-similar structures. Our main findings were summarized in a previous work.[5] Our observations confirmed the anomalous behavior of the density of states, and the existence of localized states, whereas the self-similarity of mode patterns was directly observed by means of a laser probing technique.

The purpose of the present paper is twofold. On the one hand, we shall discuss more extensively some aspects of the theoretical model, with special emphasis on the continuous character of the medium, while on the other hand we shall present some new insights and conclusions obtained from a comparison of the model, the numerical simulations, and the experimental results. We shall see that by considering a continuous medium the model leads to novel results not shared by the more common discrete or lattice models, as for instance the presence (due to higher harmonics) of multiple regions with anomalous DOS.[5] These results are not only interesting on their own, in connection with the problem of propagation and localization of classical waves in random media, but they may also be relevant to electronic transport problems.

In Sec. II we present a short introductory overview of the scaling concepts generally useful for describing fractons. In Sec. III we introduce our model structure and discuss the general behavior of the frequency spectrum for this continuous hierarchical system on a theoretical basis. This turns out to be a rather complex issue, in which both geometry and coupling between the different media play a crucial role. Section IV describes the numerical techniques used for computing eigenfrequencies and eigenmodes of our structure. We discuss the properties of localization and self-similarity, and compare results with the findings of the previous section. With the help of computer simulations we also analyze the effect of

geometrical disorder. Finally, in Sec. V, we discuss our conclusions and some general implications of our results.

II. PROPERTIES OF FRACTONS

Scale invariance of fractal structures implies the absence of any characteristic length. It is therefore assumed that on a fractal all the physical quantities behave as powers of the relevant length scale for the considered quantity:

$$Q(l) \approx l^{\alpha}.$$

Actually, real systems are fractal only within a certain range of lengths. The bounds of this range, say r and R, are therefore the lengths at which the physical properties of the system cross over to a nonfractal regime. Since r and R are now the only characteristic lengths, they will appear in the expression of Q through their ratio to l:

$$Q(l) = l^{\alpha} \cdot f(l/r) \cdot g(l/R). \tag{1}$$

In the fractal regime f and g are slowly varying functions of l, so that the power term becomes the leading one. On the other hand, when l lies outside these bounds, the properties of the system become weakly dependent on l, $Q(l) \approx$const, implying

$$f(r/l) \simeq (r/l)^{-\alpha} \quad \text{when } l \ll r,$$

and

$$g(R/l) \simeq (R/l)^{-\alpha} \quad \text{when } l \gg R.$$

Thus the characteristic exponent α also determines the properties of the system in the homogeneous regime as a function of the crossover length.

Harmonic excitations of fractals have been widely investigated during the past few years, both theoretically and experimentally.[6,4] They have been shown to exhibit essentially localized states, termed fractons.[2] It is assumed that the frequency ω of fractons behaves as

$$\omega \simeq l_{\omega}^{-d_{\omega}}, \tag{2}$$

where l_{ω} is a characteristic length of the excitations, and d_{ω} is the corresponding scaling exponent (with the minus sign for later convenience). An implication of Eq. (2) is that the modes become those of the normal regime when ω falls outside the interval $[\omega_{\text{inf}}, \omega_{\text{sup}}]$, with $\omega_{\text{inf}}, \omega_{\text{sup}}$ given by

$$\begin{aligned} \omega_{\text{inf}} &\propto R^{-d_{\omega}}, \\ \omega_{\text{sup}} &\propto r^{-d_{\omega}}, \end{aligned} \tag{3}$$

and in this case the characteristic length l_{ω} assumes the usual meaning of a wavelength. Harmonic excitations can be mathematically related to a random walk on the structure, and this allows us to express d_{ω} as a function of the random walk dimension d_W.[2,3]

As a direct consequence of Eq. (2) and of the self-similarity of the structures, it can be shown that the DOS can also be expressed as a power law:

$$g(\omega) \simeq \omega^{\tilde{d}-1}. \tag{4}$$

$\tilde{d}$ is called spectral dimension, and can be less than or equal to the Euclidean dimension. This dimension $\tilde{d}$ has also been shown to be related to d_{ω} and the fractal dimension D of the structure through the expression[2,3]

$$\tilde{d} = \frac{D}{d_{\omega}}. \tag{5}$$

Actually the density of states is a highly singular function of frequency and $\tilde{d}$ only describes its smooth behavior, and is therefore a useful approximation for computing integral quantities such as specific heat and thermal conductivity.[2] Equation (4) has been verified by experiments on solids that are thought to possess a fractal structure,[4] and by numerical simulations on both random and deterministic structures,[6] but the values found for $\tilde{d}$ do not always satisfy Eq. (5) which seems to work only for relatively simple models.[7]

Investigations of the spatial behavior of modes have not yet yielded a coherent picture of their properties. Experimental[4] and numerical[8] work has confirmed that d_{ω} actually controls the scaling of the crossover frequencies [Eq. (3)] and in this respect l_{ω} can be thought of as a sort of correlation length for fractons. But its definition [Eq. (2)] in the fractal regime is far from clear. Numerical simulations have shown that fractons usually exhibit highly irregular shapes, and procedures aimed at extracting their significant parameters must be carefully defined, in order to avoid contradictory results. A typical example concerns their localization properties. It has been suggested that fractons are superlocalized, i.e., that their decay is faster than exponential. Much theoretical work has been done in order to clarify this point, but results are still controversial (see, e.g., Refs. 8–10), depending on the way computations have been performed.

The natural interpretation of l_{ω} as a localization length, suggested since its introduction, has been confirmed by numerical work,[8] but at the same time l_{ω} has been shown to be a highly fluctuating quantity, being therefore meaningful only in a statistical sense and not for individual fractons.[11] Indeed it has been proposed that, due to the peculiarity of fractals, l_{ω} represents at the same time three fundamental lengths typical of the dynamics of fractons,[12] namely the localization length, the scattering length, and the dominant wavelength, but this hypothesis is still the subject of much discussion.[13]

Studies on deterministic fractals have shown a richer spectrum of modes.[14] In particular, aside from localized modes, a family of *hierarchical* modes also exist. These are extended modes supported by a Cantor set spectrum, which possess a whole hierarchy of localization lengths (related to the fact that they are expressed by means of families of polynomials). Similar spectra have also been found in hierarchical systems,[15] with modes having powerlike autocorrelation functions, sometimes called *critical* modes. This emphasizes some common features in the dynamics of self-similar systems (irrespective of the way in which this self-similarity is realized, in number or in strength of the interactions).

III. MODEL AND DOS

A. The model

The one-dimensional model structure is based on the construction of a triadic Cantor set.[1] By alternating elements of two different media, A and B, the sequence:

$$A$$
$$ABA$$
$$ABA\ BBB\ ABA$$
$$ABA\ BBB\ ABA\ BBBBBBBBB\ ABA\ BBB\ ABA$$
$$\ldots\ldots$$

can be constructed. A self-similar structure is then generated, with lower and upper crossover lengths determined by the size of the smallest elements and of the whole structure, respectively (for a sketch of the sample see Fig. 1 of Ref. 5). In the rest of the article we shall be concerned with scalar bulk excitations of this structure, propagating perpendicularly to the interfaces. It might seem natural to choose the same size, a and b, for the smallest elements of both media. However, as our aim is the study of the vibrational properties of the structure, it is much better to fix a and b in such a way that the two kinds of elements, when taken separately, resonate at the same characteristic frequency, ω_0. Denoting v_a and v_b the (constant) sound velocity in the respective media, this choice sets the value of the ratio of the smallest sizes to

$$\frac{a}{b} = \frac{v_a}{v_b}. \tag{6}$$

A different choice of these parameters has the effect of introducing more than one characteristic frequency in the system. This fact, besides making things more complex, can also suppress evidence of self-similarity in the spectrum.[16]

Another important factor is the acoustic mismatch between the two media. It is clear that in the limiting case of two media with the same acoustic characteristics the whole structure becomes homogeneous, with extended states and constant DOS. In the opposite case of complete decoupling, each element vibrates on its own, giving rise to a set of trivially localized degenerate modes at ω_0.

B. Main properties of the frequency spectrum

In order to derive the density of states and the spectral dimension, let us consider our model at a given generation N. It is made by

$$n_p = 2^{N+1} - 1$$

coupled resonators having ω_0 as a common eigenfrequency, constituted by alternating homogeneous sequences of type A or B. Sequences of type A are made of elements of length a and therefore resonate at ω_0 and higher harmonics. Sequences of type B are made of 3^k consecutive elements of length b, where k is an integer that ranges from 1 to $N-1$. Such sequences possess ω_0 as one of their higher harmonics. Before proceeding, it is useful to notice that the whole structure may be regarded as a periodic sequence of A and B elements, where a suitable number of A elements have been substituted by B elements that play the role of "defects" in an otherwise regular lattice. This point of view makes it easier to derive an analytical expression for the spectral exponent of the system in the limit of high acoustic mismatch, and we shall see that it will allow for a natural interpretation of the different spectral regions.

In this model the coupled oscillators are expected to give rise to n_p extended modes (phonons) resulting from the splitting of the degenerate starting frequencies, $\omega = 0$ and $\omega = \omega_0$. Since the total number of elementary resonators in the system is $n = 3^N$, we expect to have

$$n_f = n - n_p = 3^N - 2^{N+1} + 1$$

"impurity" modes, which actually are the fractons of our model. These arise from modes belonging to sequences composed of multiple B's. In an Nth generation set, there are $2^{N-(k+1)}$ sequences composed of 3^k consecutive B's, with $3^k - 1$ modes of frequency lower than ω_0. Thus the total number of these modes is

$$\sum_{k=1}^{N-1} 2^{N-(k+1)} \cdot (3^k - 1) = 3^N - 2^{N+1} + 1,$$

which is, as expected, equal to n_f.

At this stage, the system has therefore two distinct kinds of spectra of relative weights

$$W_p = \frac{1}{3^N}(2^{N+1} - 1),$$
$$W_f = 1 - \frac{1}{3^N}(2^{N+1} - 1),$$

and we see that in the limit $N \to \infty$ the phonon spectrum has vanishing weight.

Having determined the total number of fracton and phonon states, let us now proceed to see how they are distributed in the frequency domain (Fig. 1). Imposing the condition expressed by Eq. (6), the periodic system without "defects" would present only one phononic gap

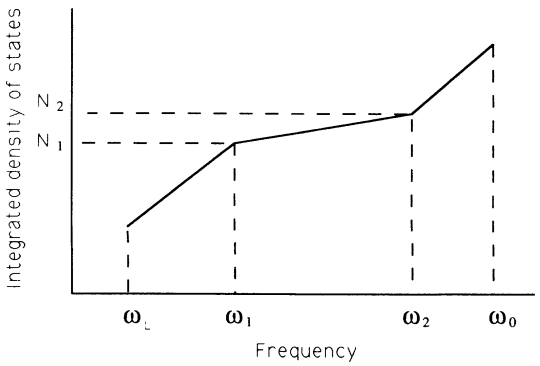

FIG. 1. Schematic integrated DOS showing the relevant frequencies ω_L, ω_1, ω_2, ω_0 (see text).

at the center of the spectrum, with band edges given by[17]

$$\omega_1 = \omega_0 - \frac{\omega_0}{\pi} \arccos M, \tag{7}$$

$$\omega_2 = \frac{\omega_0}{\pi} \arccos M, \tag{8}$$

where

$$M = \frac{|\, z_a - z_b \,|}{z_a + z_b},$$

with $z_i = \rho_i v_i$ the elastic impedance of the medium, and ρ_i its density ($i = a, b$). Fracton modes are mainly distributed in this gap but $2n_r$ of these fall in the phonon bands. We shall call them resonances. Their number can be approximately evaluated and is a function of M and N.

For the more interesting case of a large mismatching ($z_a/z_b \ll 1$), Eqs. (7) and (8) become (see Appendix A):

$$\omega_1 \simeq \alpha\omega_0, \tag{9}$$

$$\omega_2 \simeq (1-\alpha)\omega_0, \tag{10}$$

with

$$\alpha = \frac{2}{\pi\sqrt{(z_b/z_a)}},$$

and the number of resonating fractons is (see Appendix B)

$$n_r \simeq 3\alpha\left(3^{N-1} - 2^{N-1}\right).$$

The same number of fractons have frequencies between ω_2 and ω_0, while the number of fractons n_g in the phononic gap is

$$n_g \simeq 3(1-2\alpha)\left(3^{N-1} - 2^{N-1}\right).$$

We can thus distinguish three zones in the spectrum below ω_0 (see Fig. 1). Letting ω_L be the lowest nonzero frequency allowed for a system of a particular size, we have

$$N_1 \simeq n_p/2 + n_r \text{ modes for } \omega_L \lesssim \omega \lesssim \omega_1,$$
$$n_g = n_f - 2n_r \text{ modes for } \omega_1 \lesssim \omega \lesssim \omega_2,$$

and

$$n_p/2 + n_r = N_1 \text{ modes for } \omega_2 \lesssim \omega \lesssim \omega_0.$$

The total number of modes having frequency lower than ω_2 is $N_2 \simeq N_1 + n_g$, and assuming a power law behavior for the density of states in all these three ranges, the value of the spectral exponent in the fracton region is given by

$$\tilde{d} = \frac{\ln\left(\frac{N_2}{N_1}\right)}{\ln\left(\frac{\omega_2}{\max(\omega_1,\omega_L)}\right)}, \tag{11}$$

where max denotes the highest of the values in parenthesis and depends on the generation and on the parameters of the system. According to the above expression:

$$\frac{N_2}{N_1} \approx \frac{3\,(1-\alpha)\left(3^{N-1} - 2^{N-1}\right) + 2^N - 1/2}{3\alpha\,(3^{N-1} - 2^{N-1}) + 2^N - 1/2},$$

and

$$\frac{\omega_2}{\max(\omega_1,\omega_L)} \approx \frac{(1-\alpha)}{\max(\alpha, 3^{-N})}.$$

For N large enough we can retain only the largest terms, obtaining

$$\tilde{d} = \frac{\ln\left(\frac{(1-\alpha)+(2/3)^N}{\alpha+(2/3)^N}\right)}{\ln\left(\frac{1-\alpha}{\max(\alpha,3^{-N})}\right)}. \tag{12}$$

In fact only at finite generations is $\tilde{d}$ different from unity unless $\alpha = 0$. If evaluated using the same physical parameters for A and B as those used in the experiment[5] ($N = 4$, $z_a \simeq 2\times10^6$ kg/m^2 s, $z_b \simeq 23\times10^6$ kg/m^2 s, that is $\alpha \simeq 0.19$), the above expression yields $\tilde{d} \simeq 0.6$ which is in good agreement with numerical and experimental findings (see Sec. IV below, and Ref. 5).

IV. NUMERICAL RESULTS

A. Computational methods

We set up suitable numerical procedures which yield not only the eigenfrequencies but also the displacement patterns of modes. We made use of two equivalent techniques. The first technique is the most common and is based on the transmission and reflection coefficients at each interface between different media and allows us to obtain the transmittivity T of the system as a function of frequency ω.[18] For waves propagating along the direction perpendicular to the interfaces, the calculation requires imposing the boundary condition relating the two incoming and outgoing waves at each interface. One can, in principle, write down 2^{N+2} equations in 2^{N+2} unknown amplitudes, but a much simpler approach consists of setting to zero the amplitude of the wave entering the last interface from outside and treating the outgoing one as given datum. Thus one must recursively solve a sequence of 2^{N+1} independent equations:

$$u^+_{m+1} = M\ u^+_m + N\ u^-_m,$$
$$u^-_{m+1} = P\ u^+_m + Q\ u^-_m,$$

with $m = 1, 2, ..., 2^{N+1} - 2$ the interface label, $u^\pm_m$ the amplitudes of the outgoing and incoming waves at the corresponding interface, and the coefficients M, N, P, Q are functions of parameters of the medium, including reflection coefficients, lengths, etc. The transmittivity function of the system is equal to the square of the ratio between the last outgoing wave and the first incoming one:

$$T(\omega) = \left(\frac{u_{2^{N+1}-2}}{u_0}\right)^2.$$

This method was applied to compute the integrated density of states and the displacement patterns of the modes.[5]

The second technique is derived from dynamical transfer matrix techniques used in linear system theory.[19] For each sequence of elements, one builds a matrix of the form

$$S_i = \begin{pmatrix} \cos(k_i d_i) & \frac{1}{\omega}\frac{\sin(k_i d_i)}{z_i} \\ -\omega z_i \sin(k_i d_i) & \cos(k_i d_i) \end{pmatrix},$$

where $i = a, b$; k_i is the wave number; z_i is the acoustic impedance and d_i the length of each sequence. This matrix operates on the two-component vector $\mathbf{u_i} = (u_i, \tau_i)$, where u_i and τ_i are the values of wave amplitude and stress at one side of the ith element, yielding as output the value of $\mathbf{u}_i$ at the other side. This value is the input value for the matrix S_{i+1}, and so on. Thus, the product of the matrices for the sequences A and B in the correct order yields the value of $\mathbf{u}$ at one end of the system as a function of its value at the other end. One can choose the desired initial conditions as a starting value for $\mathbf{u}$ and verify for which value of ω the correct boundary conditions are obtained. This technique is not substantially different from the first one, but allows a more direct computation of the wave number Q of the infinite periodic structure having the system as unitary cell. With S the matrix for a cell of this kind of length L, it can be shown that

$$\cos(QL) = \frac{1}{2}\mathrm{Tr}(S),$$

where Tr is the trace operator, and therefore the allowed frequencies must meet the condition $|\ \mathrm{Tr}(S)\ | \leq 2$. The knowledge of such dispersion curves is useful in identifying localized states, which correspond to the flat branches.

B. Frequency spectra

Figure 2 shows a log-log plot of cumulated DOS for the second to fifth generation of our Cantor-like structure. It has been computed using the dynamical matrix technique, with the same parameters for A and B as those used in the experiment,[5] that is $z_a \simeq 2 \times 10^6$ kg/m^2 s, $v_a = 1700$ m/s, $a \simeq 0.45$ mm, and $z_b \simeq 23 \times 10^6$ kg/m^2 s, $v_b = 3000$ m/s, $b = 0.8$ mm. Each plot has been obtained from the dispersion curve of an infinitely replicated Cantor unit cell. We have associated a single state of the single isolated Cantor cell to each band of the infinite structure (for this reason each state in the graph is represented by a segment of a curve instead of a point). For comparison, we also show the cumulated DOS of a periodic structure, made by alternating 46 A and 45 B layers with the same parameters. As expected, it can be seen that there is a change in the slope of the curve in the frequency range corresponding to the gap interval of the periodic structure, delimited by the frequencies $\omega_1/2\pi = f_1 \simeq 330$ kHz and $\omega_2/2\pi = f_2 \simeq 1600$ kHz. This is the range in which only fracton modes are expected. For the fourth generation, a best fit yields $\tilde{d} = 0.63$ as spectral exponent within this range, while in the ranges corresponding to the bands of the periodic structure the slope is always very close to one. The higher the generation, the more states one finds in the fracton range. They cluster into quasidegenerate groups, corresponding to modes mainly localized in portions of the structure of similar geometry, with the exception of those isolated states not belonging to the previous generations.

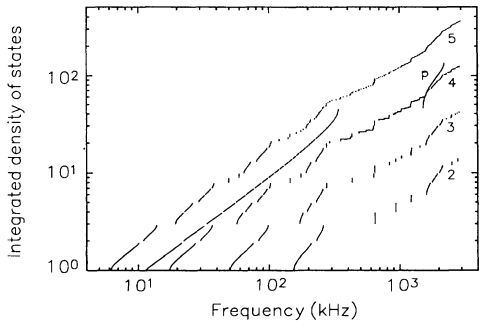

FIG. 2. Integrated DOS of the Cantor-like structure, for generations 2 – 5. The continuous lines marked "p" correspond to a periodic structure formed by alternating elements with the same size as the smallest elements of the Cantor-like structure.

Owing to the continuity of the media, there is no upper frequency limit as in discrete systems; on the contrary, the frequency spectrum exhibits bands of modes at high frequencies which have similar characteristics to the bands at low frequency. For example, with $f_0 = \omega_0/2\pi = 1875$ kHz the resonance frequency of the single basic element, the DOS between $f = f_0$ and $f = 2f_0$ is the same as between $f = 0$ and $f = f_0$, with the fracton gap starting at $f = f_0 + f_1$ and ending at $f = f_0 + f_2$, and so on. This remarkable feature of continuous systems shows that there can exist multiple crossovers from localized to extended states whenever the continuum approximation holds. The possible consequences would be worth investigating. Indeed, the same behavior can be expected to hold for electrons in suitable heterostructures, with consequences for their conductance and other relevent properties. Another important feature of these kinds of systems is that, as discussed in the previous section, many fracton modes fall in the bands of extended modes. These resonant modes allow transitions from localized to extended states with energetic costs close to zero, possibly modifying the transport properties.[22] Experimental evidence for these resonant modes has been presented elsewhere.[23]

C. Displacement patterns of modes

Numerical simulations allow us to make evident some properties of the displacement patterns of normal modes. We are mainly concerned here with properties of localization and self-similarity.

The patterns in Fig. 3(a) (as well as in Figs. 4 and 5 of Ref. 5) belong to some modes of the fracton range. They look like localized modes, at least locally, but it can be observed that they are actually extended. In fact, if an excitation can survive at a certain frequency in some portion of the structure, it will also be present in other places owing to the fact that, if the number of generations is large enough, it is always possible to find a portion exactly similar to the given one. This mechanism gives origin to modes of hierarchical nature, with properties that are different from those characteristic of

other systems lacking translational invariance. Nevertheless, this peculiar kind of extended mode is based on the rigorous similarity and hierarchy of the different portions of the structure, with a mechanism of tunneling for the wavelike excitations, a mechanism which is known to be highly unstable.[20] This means that hierarchical states can be destroyed by small perturbations. Therefore they are not likely to survive in real systems which are only self-similar in a statistical sense, and we can think of them as effectively localized modes. Hierarchical states are supposed to scale with frequency in a self-similar way and our model satisfies this requirement (see Fig. 5 in Ref. 5 where three modes display self-similar patterns, and their frequencies are in a ratio of $\approx 1/3$ from one another).

Figure 4(a) shows the computed dispersion curve of the fourth generation in the frequency range 1900 − −2200 kHz which is interesting because both localized and extended modes are present. Q represents the lattice wave vector of the structure, in the sense that it is the wave vector of the system obtained by periodically repeating the whole structure with period L ($Q = 2n\pi/L$). Some branches, like those labeled with 2 and 4, look nearly flat, and are therefore expected to exhibit (hierarchically) localized modes. On the contrary, branches like those labeled 1 and 3 have a significant dispersion, characteristic of extended modes. The mode patterns corresponding to the labeled branches are shown in Fig. 3(a). We see that nonextended modes do indeed belong to the flat branches. We also computed $\omega(Q)$ in the fracton zone, obtaining similar results [Figs. 3(b) and 4(b)].

Finally we tried to verify if the interpretation of l_ω as a sort of wavelength in the fracton dispersion law, Eq. (2), holds in our case. For modes in the fracton regime we now define an effective wavelength as the ratio of the length in which the mode is locally localized, to half the number of its nodes. The dispersion law constructed in this way follows a linear behavior on a log-log scale, with slope d_ω close to one.[5] From Eq. (5) we then obtain $\tilde{d} \approx D$ as the spectral exponent for these regions, which agrees numerically with the one directly derived from the slope of the DOS in Fig. 2.

D. Fine structure of the spectrum and influence of disorder

The properties of the spectrum derived in Sec. III are valid for a much larger class of systems than the one discussed so far. In fact, the order of the B-type sequences

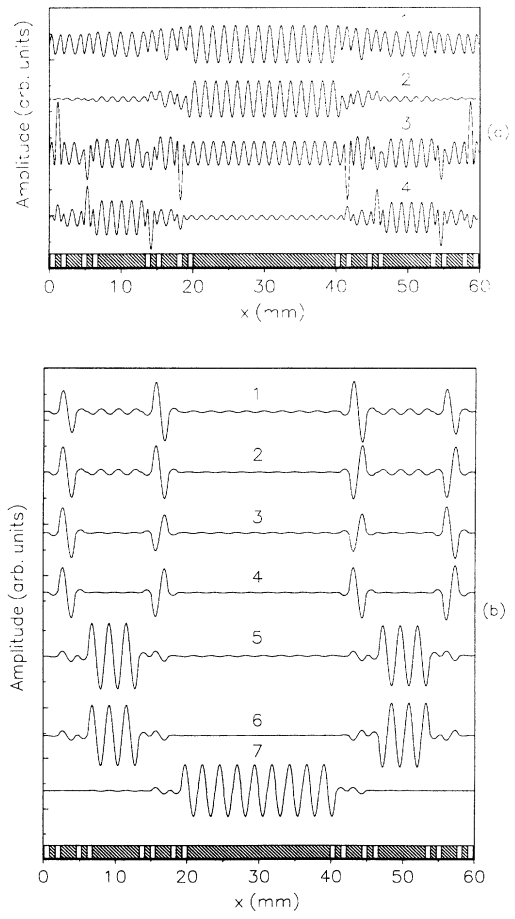

FIG. 3. (a) Some displacement patterns of localized hierarchical modes marked in Fig. 4(a); (b) displacement patterns for modes in the branches marked in Fig. 4(b), showing localized and nonlocalized modes.

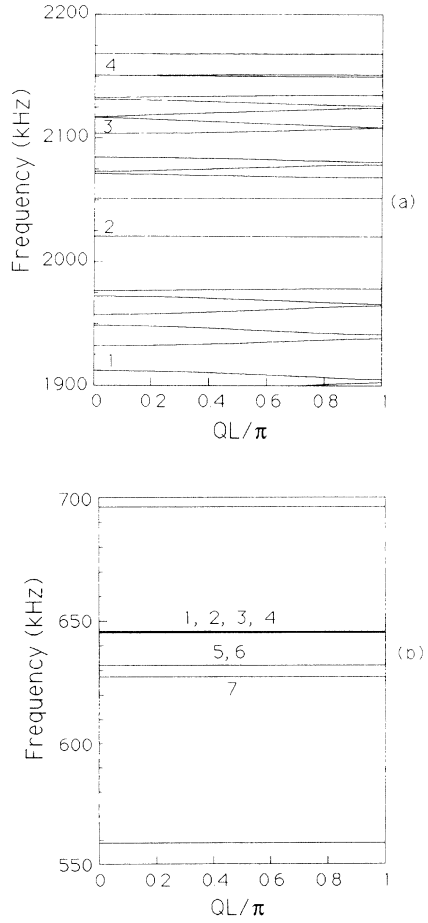

FIG. 4. Dispersion in the fracton region (a) and in a frequency range showing both dispersive and nondispersive branches. The displacement profiles associated to the numbered modes are shown in Fig. 3.

in the discussion is not important, as long as the acoustic mismatch between A and B is sufficiently large. In this case we may thus change the order of these sequences with no relevant changes in the DOS. We have verified this statement by numerically computing the spectrum of a number of systems in which the 2^N sequences of B-type alternate randomly with the A-type elements. Figure 5 shows the results of one such computation for a case with the same number of elements as that of the fourth generation but randomly distributed. The mode frequencies of the ordered Cantor structure are represented versus those of the disordered structure. The linear behavior shows that no substantial differences exist between them with the exception of the extended mode regions where indeed the randomization is expected to influence the interaction among modes. Similar results were obtained in the other cases.

Actually, the order of the sequences only affects the "fine structure" of the spectrum, this latter being essentially determined by the coupling among those sequences of B which would possess the same resonant frequencies, if taken as isolated resonators. Coupling removes degeneracies with a splitting dependent on its strength. In ordered structures we expect to have a hierarchy of couplings, and therefore a hierarchical distribution of splittings, whereas disorder produces a rather flat distribution. Figures 6 and 7 show these distributions for the spectra of Fig. 5. The splittings of the ordered system (Fig. 6) group around very few values, while they distribute much more uniformly in the disordered case (Fig. 7). It also can be seen that each distribution consists of two main parts. One of them, with a maximum close to zero, is due to the small splitting values and is asymmetric, with a long tail towards the positive abscissas; thus it pertains to quasidegenerate modes possessing very weak couplings, and must therefore be attributed to localized modes. The other part of the distribution is bell-shaped, centered around higher values of the splittings, and comes from stronger couplings among different regions of the system, which give rise to extended modes. Quite noticeably, the two different shapes resemble very much the ones related to the statistics of eigenvalue spacing of random matrices.[21] In this case the small splitting

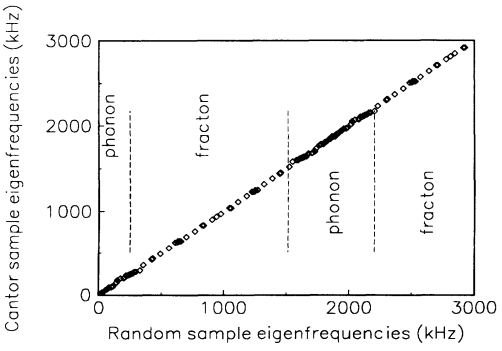

FIG. 5. Plot of the mode frequencies of a fourth generation hierarchical structure versus mode frequencies of the structure with randomly alternating B sequences.

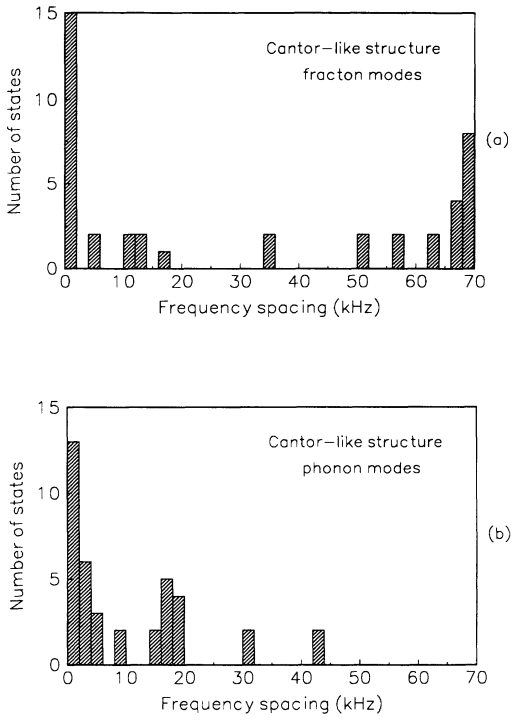

FIG. 6. Histogram of the mode splitting distribution derived from the spectrum of the Cantor ordered structure in the fracton zone (a), and in the extended mode region (b).

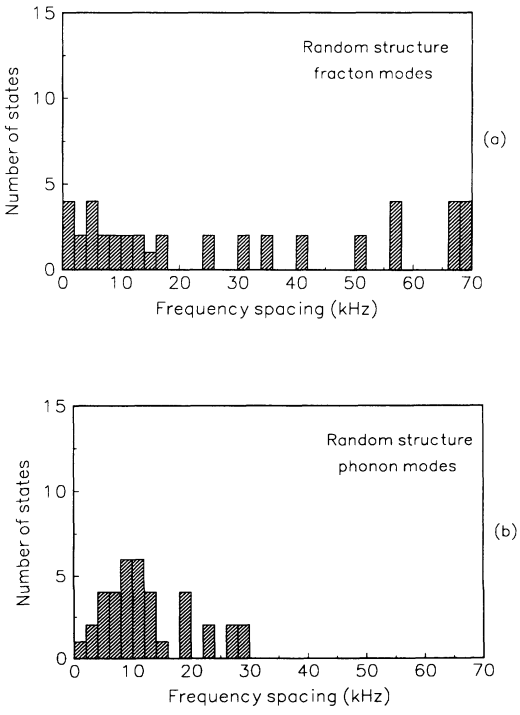

FIG. 7. Same as Fig. 6 but for a random distribution of the elements.

statistics are described by a Poisson distribution of level spacings, corresponding to uncorrelated eigenvalues with localized eigenvectors. On the contrary, the other distribution is characteristic of strongly correlated eigenvalues, which possess extended eigenstates. Along with the slope change in the DOS, this provides strong evidence for the simultaneous presence of both kinds of states in these systems. Investigation of the spatial behavior of normal modes of such disordered structures is the subject of a forthcoming publication.

V. CONCLUSIONS

We have studied the properties of the vibrational spectrum for hierarchical systems with large acoustic mismatch between the constituent homogeneous materials. We have shown that in such continuous structures the spectral dimension can be analytically predicted by means of "mode counting" arguments, provided that resonant modes are carefully taken into account. The results are in excellent agreement with previous experimental observations[5] as well as with new numerical calculations, and together with the analysis of the eigenvalue spacings and of the dispersion curves of finite size systems they provide new evidence for the existence and understanding of multiple phonon and fracton regimes in these structures.[5] Indeed, successive phonon and fracton regimes are shown to derive from higher harmonics associated with individual components of the structures. On the basis of this understanding, it was quite natural to expect that many properties of our hierarchical structure should be preserved when the sequence of the elements was modified while keeping their size and number unchanged. We have therefore undertaken a detailed analysis of the density of states, displacement patterns, and eigenvalue spacing distribution of new structures with a random distribution of the elements. The results demonstrate that the choice of the sequence does introduce interesting modifications in the "fine structure" of the spectrum, but it does not alter significantly the main picture. This allows us to extend our previous conclusions[5] to a larger class of structures, possibly closer to "real" complex materials. Moreover, we have recently found that enhanced nonlinear effects result from the interaction among localized and extended modes which is typical of the Cantor-like structures as compared to periodical and homogeneous systems of the same nature.[23] The present paper supports the idea that also these nonlinear effects may be of more general relevance.[23,24]

ACKNOWLEDGMENTS

We are grateful to M. Acciarini for expert technical assistance. This work was supported in part by CNR under Grant No. 92.01598.PF69 (Progetto Finalizzato Calcolo Parallelo).

APPENDIX A

The phononic zone center gap in binary periodic systems having $\frac{a}{b} = \frac{v_a}{v_b}$ [see Eq. (6)], is bounded by the frequencies[17]

$$\omega_{1,2} = \frac{\omega_0}{\pi} \arccos(\pm M), \tag{A1}$$

with $M = \frac{R-1}{R+1}$, $R = z_b/z_a$, and $\omega_0 = \pi v_a/a = \pi v_b/b$. In this case there are no zone boundary gaps. When $R \gg 1$, $M \approx 1 - 2/R$, and expanding Eq. (A1) to first order in $1/\sqrt{R}$ yields

$$\omega_1 \simeq \omega_0 \frac{2}{\pi\sqrt{R}}, \tag{A2}$$

$$\omega_2 \simeq \omega_0 \left(1 - \frac{2}{\pi\sqrt{R}}\right). \tag{A3}$$

APPENDIX B

As suggested at the beginning of Sec. III B, the hierarchical structure described can be considered as a periodic system made by alternating single elements of types A and B, in which a certain number of B elements have been substituted by longer B sequences, made of 3^k consecutive elements ($k = 1, 2, \ldots, N-1$, for a given generation N). In order to obtain the spectrum of this system let us look at the B sequences as isolated resonators, and assume the corresponding frequencies to be good estimates of the real ones. This can seem a rather rough approximation, but experiments and numerical simulations have shown it to work quite well in the case of high elastic mismatching ($z_b \gg z_a$). Within this approximation, a sequence of 3^k consecutive elements possesses the eigenfrequencies:

$$\frac{j^{(k)}}{3^k}\,\omega_0 \quad (j^{(k)} = 1, 2, \ldots, 3^k).$$

The last frequency ($j^{(k)} = 3^k$) pertains to the phononic band, as it is shared by all the sequences, while the others represent fractonic modes. Among the latter, the ones falling in the phononic gap of the periodic structure are only those for which

$$\omega_1 \lesssim \frac{j^{(k)}}{3^k}\omega_0 \lesssim \omega_2. \tag{B1}$$

Their total number can be evaluated within the assumed approximation. From Eqs. (A2) and (A3), condition (B1) becomes

$$j_1^{(k)} < j^{(k)} \leq j_2^{(k)},$$

with $j_1^{(k)}$ the lower closest integer to α^{3k} and $j_2^{(k)}$ the lower closest integer to $(1-\alpha)3^k$. It is seen that only about $j_2^{(k)} - j_1^{(k)}$ modes of the considered sequence have frequencies in the gap region. At the Nth generation there are 2^{N-k-1} sequences made of 3^k consecutive B elements, and k ranges from 1 to $N-1$. Thus the total number of modes in the gap is

$$n_g = \sum_{k=1}^{N-1} 2^{N-k-1}(j_2^{(k)} - j_1^{(k)}) = (1-2\alpha)(3^N - 3\cdot 2^{N-1}).$$

In the same way we get the number of fracton modes having frequency less than ω_1 (i.e., those having $j^{(k)} \leq j_1^{(k)}$):

$$n_r = \sum_{k=1}^{N-1} 2^{N-k-1}\, j_1^{(k)} = \alpha(3^N - 3 \cdot 2^{N-1}).$$

The remaining fracton modes (still n_r) have frequencies in the range between ω_2 and ω_0. The total number of modes (phonons and fractons) with frequency less than ω_1 is therefore

$$N_1 = \frac{n_p}{2} + n_r \simeq 3\alpha\left(3^{N-1} - 2^{N-1}\right) + 2^N + 1/2,$$

whereas the total number of modes up to ω_2 is

$$N_2 = \frac{n_p}{2} + n_r + n_g \simeq 3(1-\alpha)\left(3^{N-1} - 2^{N-1}\right) + 2^N + 1/2.$$

*Also at Dipartimento di Fisica, Università di Roma "La Sapienza," Piazzale A. Moro 2, 00185 Roma, Italy.

[1]B. B. Mandelbrot, *The Fractal Geometry of Nature* (Freeman, New York, 1982).
[2]S. Alexander and R. Orbach, J. Phys. (Paris) Lett. **43**, L625 (1982).
[3]R. Rammal and G. Toulouse, J. Phys. (Paris) Lett. **44**, L13 (1983).
[4]E. Courtens and R. Vacher, Proc. R. Soc. London, Ser. A **423**, 55 (1989), and references therein.
[5]F. Craciun, A. Bettucci, E. Molinari, A. Petri, and A. Alippi, Phys. Rev. Lett. **68**, 1555 (1992).
[6]R. Orbach, Physica D **38**, 266 (1989), and references therein.
[7]Itzhak Webman and Gary S. Grest, Phys. Rev. B **31**, 1689 (1985).
[8]Qiming Li, C. M. Soukoulis, and Gary S. Grest, Phys. Rev. B **41**, 11713 (1990).
[9]K. Yakubo and T. Nakayama, Phys. Rev. B **40**, 517 (1989).
[10]C. J. Lambert and G. D. Hughes, Phys. Rev. Let. **66**, 1074 (1991).
[11]A. Petri and L. Pietronero, Phys. Rev. B **45**, 12864 (1992), and references therein.
[12]S. Alexander, Phys. Rev. B **40**, 7953 (1989).
[13]See, e.g., V. Mazzacurati, M. Montagna, O. Pilla, G. Viliani, G. Ruocco, and G. Signorelli, Phys. Rev. B **45**, 2126 (1992), and references therein.
[14]R. Rammal, J. Phys. **45**, 191 (1984).
[15]See, e.g., R. Livi, A. Maritan, and S. Ruffo, Stat. Phys. **52**, 595 (1988), and references therein.
[16]V. V. Konotop, O. I. Yordanov, and I. V. Yurkevich, Europhys. Lett. **12**, 481 (1990).
[17]P. V. Santos, L. Ley, J. Mebert, and O. Koblinger, Phys. Rev. B **36**, 4858 (1987).
[18]A. Alippi, F. Craciun, and E. Molinari, J. Appl. Phys. **66**, 2828 (1989).
[19]S. Flugge, *Encyclopedia of Physics* (Springer, Berlin, 1959), Vol. 44, p. 302; C. Bernardini and C. Pellegrini, Ann. Phys. **46**, 174 (1968).
[20]G. Jona Lasinio, F. Martinelli, and E. Scoppola, J. Phys. A **17**, L635 (1984).
[21]P. Argyrakis, S. N. Evangelou, and K. Magoutis, Z. Phys. B **87**, 257 (1992).
[22]A. Alippi, G. Shkerdin, A. Bettucci, F. Craciun, E. Molinari, and A. Petri, Phys. Rev. Lett. **69**, 3318 (1992).
[23]A. Alippi, A. Bettucci, F. Craciun, E. Molinari, and A. Petri, *Proceedings of the 1991 IEEE Ultrasonics Symposium*, edited by M. Levy and B. R. McAvoy (IEEE, New York, 1991), p. 399.
[24]R. Orbach, Philos. Mag. B **65**, 289 (1992), and references therein.